Dalton Transactions

PAPER

View Article Online
View Journal | View Issue

Cite this: *Dalton Trans.*, 2018, **47**, 16139

pH-Control as a way to fine-tune the Cu/Cu_2O ratio in radiation induced synthesis of Cu_2O particles†

Zhuofeng Li, *[a] Inna L. Soroka, [a] Fanyi Min[a,b] and Mats Jonsson[a]

Received 17th July 2018,
Accepted 26th October 2018

DOI: 10.1039/c8dt02916d

rsc.li/dalton

In this work we have optimized the γ-radiation induced synthesis of Cu–Cu_2O particles from aqueous $CuSO_4$ solution by investigating the effect of pH. The obtained precipitate was analyzed by XRD and SEM techniques. The results indicated that at solution pH lower than 3.75, quasi-spherical Cu agglomerates can be formed while at pH higher than 4.40 only octahedron-shaped Cu_2O particles are produced. At solution pH in the range from 3.75 to 4.40, a Cu–Cu_2O mixture is produced. It was found that the relative amount of Cu_2O in the Cu–Cu_2O precipitate increases with pH in the studied range. The influence of solution pH on the Cu/Cu_2O ratios in the product can be explained on the basis of pH-dependent competition kinetics between the reactions leading to either Cu or Cu_2O formation. As a consequence, the composition and morphology of the Cu–Cu_2O precipitate can be tuned by controlling pH of the aqueous $CuSO_4$ solution during the γ-radiation induced synthesis.

Introduction

Metal and metal oxide particles have received increasing attention during the last decades due to their catalytic,[1] magnetic,[2] conductive[3] and optical[4] properties. Among these materials, cuprous oxide (Cu_2O) has been investigated extensively since it is an important p-type semiconductor with a band gap of 2.2 eV.[5–9] Cu_2O particles have potential applications in solar energy conversion,[10] photocatalysis,[5] biosensing[11] and organic synthesis.[12] The expanding application of Cu_2O requires the materials to be produced with well controlled size, shape, morphology and composition. One of the possible routes to synthesis of Cu_2O is to precipitate it from solution by changing the redox potential. Kumar *et al.*[13] prepared Cu_2O nanocubes with a hierarchical structure by a one-pot synthesis method employing polyethylene glycol and glucose as a structure-directing agent and reductant, respectively. Xu *et al.*[14] synthesized octahedral Cu_2O crystal by reducing copper hydroxide with hydrazine. Yu *et al.*[15] prepared CuO/Cu_2O composite hollow microspheres with controlled diameter and composition by hydrothermal synthesis using $Cu(CH_3COO)_2{\cdot}H_2O$ as a precursor.

In the current study, a γ-radiation induced method is used to produce Cu_2O particles. The use of ionizing radiation in synthesizing particles has several advantages compared to other methods. Among other things, the method can be used to synthesize both organic and inorganic particles in a process where the use of harmful chemicals can be avoided and the synthesis scheme becomes quite simple.[16–20] Gold nanoparticles,[21] Palladium catlysts[22] and Pt/CNTs catalysts[23] have been produced by γ-radiation induced synthesis methods. Though most of the products were noble metal particles, there were some studies about preparing metal oxides by this method, such as MnO_2,[24] Fe_2O_3,[25] UO_2,[26] Co_3O_4 [20] and Cr_2O_3.[27,28] There are several studies about γ-radiation induced synthesis of Cu_2O particles. He *et al.*[29] investigated the size-controlled preparation of Cu_2O octahedron nanocrystals by γ-irradiation and found that the average edge of the octahedron Cu_2O nanocrystals varied from 45 to 95 nm as a function of the γ-radiation dose rate. Furthermore, Liu *et al.*[30] reported a shape controlled synthesis of Cu_2O particles, such as eight-pod cubic, six-armed star-like, octahedral and spindle-like structure, by γ-irradiation with cetyltrimethylammonium bromide (CTAB) as a nucleation and growth controller.

It is well known that the pH value of the precursor solution can have a significant effect on the structural properties of the particles formed in aqueous systems.[31–36] Also, solution pH influences the yield of the obtained Cu precipitate.[37]

The aim of the current study is to investigate the influence of pH of the Cu precursor solution on the composition, conversion and morphology of the Cu–Cu_2O precipitate obtained

[a]*Applied Physical Chemistry, School of Engineering Sciences in Chemistry, Biotechnology and Health, KTH Royal Institute of Technology, SE-100 44 Stockholm, Sweden. E-mail: zhuofeng@kth.se; Tel: +46 722964921*
[b]*School of Chemical Science, University of Chinese Academy of Sciences, 100049 Beijing, P. R. China*

†Electronic supplementary information (ESI) available. See DOI: 10.1039/c8dt02916d

by γ-radiation induced synthesis, as well as to work out the optimal conditions for synthesis of crystalline Cu_2O without Cu admixtures.

Experimental

Radiation induced synthesis method

Radiation-induced formation of particles in solution is in general based on reactions between solvent radiolysis products and solute precursors. To produce metal or metal oxide particles, metal ions are usually used as solute precursors. In this work, water is used as solvent for the reaction system. Upon absorption of ionizing radiation water is decomposed into oxidizing and reducing species:[24]

$$H_2O \xrightarrow{\gamma\text{-radiation}} e^-_{aq}, H_3O^+, H^\bullet, OH^\bullet, H_2, H_2O_2. \quad (1)$$

The chemical change induced by γ-irradiation can be quantified *via* the radiation chemical yield or *G*-value which is the number of moles of a given species produced or consumed per absorbed Joule of radiation energy [mol J^{-1}].[24] Among the water radiolysis products, e^-_{aq} and $OH^\bullet$ are produced with the highest yield at pH 7 in γ-irradiated solutions.[24] The *G*-values of e^-_{aq} and $OH^\bullet$ are both 0.28 μmol J^{-1} at times >10^{-6} s (ref. 24) after the initial absorption of the radiation energy. The *G*-values are pH independent in pH range from 3 to 13.[38] The hydrated electron, e^-_{aq}, is a very strong reductant, $E^0(H_2O/e^-_{aq})$ = −2.87 V *vs.* SHE, capable of reducing most metal ions to lower valence states.[39] It acts as the most effective reducing agent in the system, the rate constant of the reaction between e^-_{aq} and Cu^{2+} ions is 8.2 × 10^9 dm^3 mol^{-1} S^{-1}.[40] $OH^\bullet$ is a very strong oxidant capable of oxidizing metal ions to a higher oxidation states.[24] For γ-radiation induced synthesis, the redox conditions of solution can be tuned to either oxidizing or reducing condition by adding radical scavengers prior to irradiation. The scavengers can react with undesired radicals and sometimes also convert them into other radicals with the desired properties. In the present work, the reducing route was selected to produce Cu_2O particles in Cu^{2+} solution. This was achieved by using isopropanol which can react with $OH^\bullet$ and produces the reducing radical $(CH_3)_2CO^\bullet H$, $E^0((CH_3)_2CO/(CH_3)_2CO^\bullet H)$ = −1.8 V *vs.* SHE:[41]

$$(CH_3)_2CHOH + OH^\bullet \rightarrow (CH_3)_2CO^\bullet H + H_2O. \quad (2)$$

Furthermore, *via* the reaction (2) the isopropanol scavenges the oxidizing radical $OH^\bullet$ and produce same amount of reducing radical $(CH_3)_2CO^\bullet H$. Hence, the total *G*-value for reducing radicals in this system will be doubled (G(red) = $G(e^-_{aq})$ + $G(OH^\bullet)$) and equal to 5.6 × 10^{-7} mol J^{-1}.

Synthesis condition

In a typical preparation, the aqueous solution (Millipore Milli-Q) contained 0.01 M $CuSO_4{\cdot}5H_2O$ (Merck, 99.8%), 2.0 M isopropanol (Sigma-Aldrich, 99.9%) and 0.50 M CH_3COOH/CH_3COO^- buffer. 0.008 M sodium dodecyl sulfate (SDS, Fluka, 99.0%) was used as surfactant in every experiments. The CH_3COOH/CH_3COO^- ratio was varied to adjust pH between 3.75 and 4.40. The solutions were purged with high purity nitrogen (Standmollen, 99.999%) for 30 min to remove oxygen from the solution prior to irradiation. Thereafter, the solutions were irradiated using Cs-137 γ source at a dose rate of 0.124 Gy s^{-1} for 20 hours. The total absorbed dose was 8.9 kGy for each sample. After irradiation, the obtained red precipitate was washed with deionized water several times and filtered.

Characterization

Optical absorption spectra were acquired using a JASCO V-730 spectrophotometer to measure the Cu(II)-concentration in the copper sulfate solutions before and after irradiation. The intensities of the absorption peaks at a wavelength of 777 nm typical for Cu^{2+}_{aq} were used.[42] Powder X-ray diffraction (XRD) patterns of synthesized particles were recorded by a PANalytical X'Pert PRO diffraction system using Cu Kα radiation (λ = 1.54 Å) in Bragg–Brentano geometry. XRD scans were recorded in 2θ range from 5° to 95° with a step of 0.01°. Scanning electron microscopy (SEM) and energy dispersive spectroscopy (EDS) were performed using a VP-SEM S3700N setup.

Results and discussion

The powder X-ray diffraction patterns of the precipitated particles produced at the different pH-values of the copper sulfate solutions are shown in Fig. 1. It should be noted that the solution pH before and after irradiation was found to be similar within the uncertainty of 0.05 pH-units. The pH values of the solutions are denoted in the figure. As seen in the figure, for the sample at pH 3.75, only the diffraction peaks attributed to metallic Cu were detected.[43–45] While for the sample synthesized at pH 3.85, the characteristic peaks of Cu_2O are observed[13] in addition to those which belong to Cu. The two

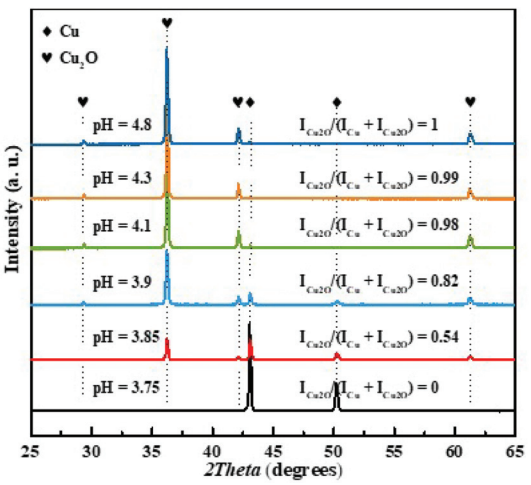

Fig. 1 XRD patterns of the Cu–Cu_2O powders synthesized at different pH values, rhombus and hearts denote XRD peaks for Cu and Cu_2O, respectively.

different copper species were also verified by SEM-EDS mapping, see Fig. S1.† With further increase of solution pH, the intensities of the diffraction peaks corresponding to Cu gradually decrease while those corresponding to Cu_2O increase. Finally, at pH 4.4 only XRD peaks which belong to Cu_2O are detected. To be able to quantify and compare the results from XRD measurements, the ratio $I_{Cu_2O}/(I_{Cu} + I_{Cu_2O})$ was introduced where I_{Cu_2O} and I_{Cu} represented the sum of integral intensities of XRD peaks for Cu_2O ((110), (111), (200) and (220) planes) and for Cu ((111) and (200) planes), respectively. Note, that the suggested ratio represented the relative content of Cu_2O in the Cu–Cu_2O crystalline phase precipitate. The XRD results were summarized in Table S1† and Fig. 3(a). Thus, by varying the copper sulfate solution pH without changing other synthesis parameters, one can tune the composition of the precipitate obtained by γ-radiation induced synthesis.

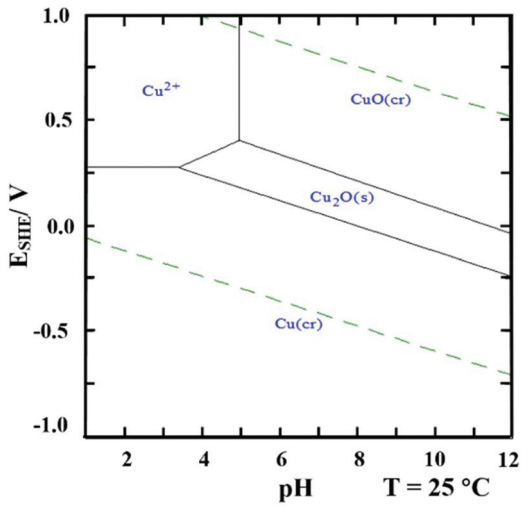

Fig. 2 E-pH diagram showing predominant phases in the Cu–H_2O system (0.01 M Cu^{2+} aqueous solution).

The effect of pH can be understood from the E-pH diagram[46] of the Cu–H_2O system with 0.01 M Cu^{2+} shown in Fig. 2. As seen in the diagram at solution pH < 3.5, only metallic copper can be formed when lowering the potential, $Cu^{2+} \rightarrow Cu^0$. At 3.5 < pH < 5 there is a potential interval where Cu_2O(s) is stable. However, upon further reduction of the potential Cu^0 is formed.

To elucidate the mechanism of Cu_2O formation, we plotted the ratios of the integral intensities of the XRD peaks $I_{Cu_2O}/(I_{Cu} + I_{Cu_2O})$ as a function of solution pH, see Fig. 3(a). Also the conversion of Cu^{2+} (ΔCu^{2+}), *i.e.*, the change in Cu(II)-concentration upon irradiation, is plotted as a function of solution pH as well, see Fig. 3(b). As seen in Fig. 3(a) the ratio of $I_{Cu_2O}/(I_{Cu} + I_{Cu_2O})$ changes gradually from 0 to 1, indicating co-existence of pure crystalline Cu and Cu_2O phases in the solution in the pH range used in the experiments. In the pH range from 3.75 to 4.0, the Cu–Cu_2O precipitate can be obtained. It is also clear that the Cu^{2+} conversion increases gradually with solution pH and its value doubles when solely Cu_2O forms.

Cu^{2+} will be reduced to form Cu_2O through the following reactions (3)–(5).[42,47] Metallic Cu particles could either be produce by two consecutive one-electron transfer steps from Cu^{2+} *via* Cu^+ to Cu^0, reactions (3) and (6),[40] or through disproportionation of Cu^+, reaction (7):

$$Cu^{2+} + e^-_{aq} \text{ or } (CH_3)_2CO^{\bullet}H \rightarrow Cu^+ \quad (3)$$

$$Cu^+ + H_2O \rightarrow CuOH + H^+ \quad (4)$$

$$2CuOH \rightarrow Cu_2O + H_2O \quad (5)$$

$$Cu^+ + e^-_{aq} \rightarrow Cu^0 \quad (6)$$

$$2Cu^+ \rightarrow Cu^0 + Cu^{2+} \quad (7)$$

The change in $I_{Cu_2O}/(I_{Cu} + I_{Cu_2O})$ with pH implies that there is a pH-dependent competition between the reaction yielding Cu_2O (4) and the reactions yielding Cu (6) and (7), where reaction (4) is favored at higher pH. The apparent pH-effect on the

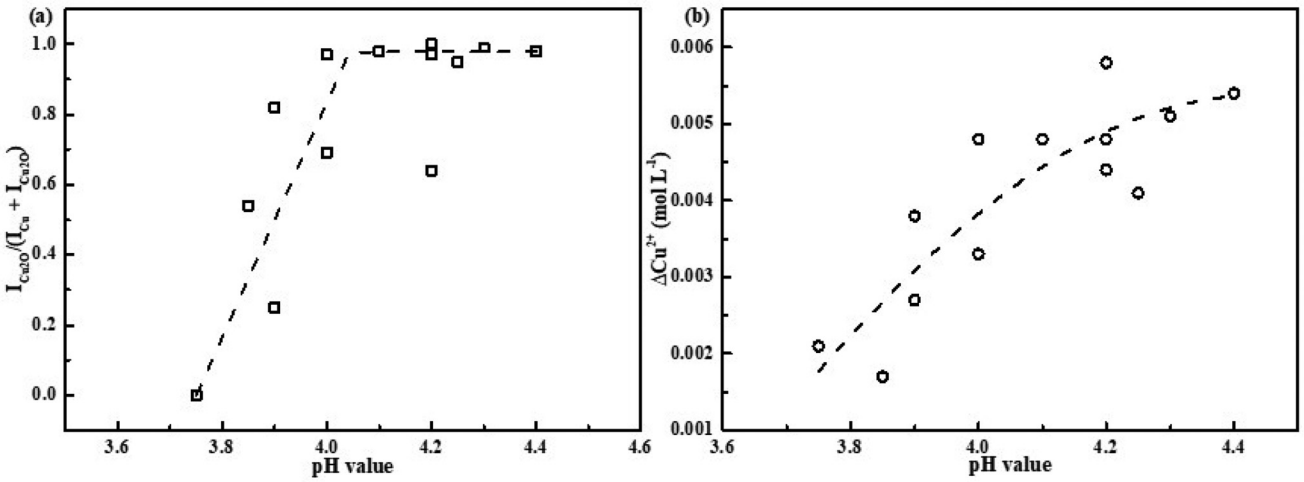

Fig. 3 The ratios of relative XRD intensities $I_{Cu_2O}/(I_{Cu} + I_{Cu_2O})$, $I_{Cu_2O}/(I_{Cu} + I_{Cu_2O})$ was the ratios of integral intensities of XRD peaks, which I_{Cu_2O} and I_{Cu} represented the sum of integral intensities of peaks for Cu_2O ((110), (111), (200) and (220)) and for Cu ((111) and (200)), respectively. (a) and Cu^{2+} conversion yield ΔCu^{2+} (b) as a function of solution pH, dash lines are guide for eyes.

Cu^{2+} conversion at the given absorbed dose directly follows from this since two electrons are required to convert Cu^{2+} to Cu while only one electron per Cu^{2+} is required to produce Cu_2O according to proposed scheme. This is confirmed by the results shown in Fig. 3.

The influence of scavenger (isopropanol) concentration on Cu_2O formation was also investigated and the results are shown in Fig. 4. As the results indicate, the ratio of $I_{Cu_2O}/(I_{Cu} + I_{Cu_2O})$ increases with increasing isopropanol concentration in the range 0.5 M to 1.0 M. This could partly be attributed to hydroxyl radicals reacting with the buffer in competition with the desired reaction with isopropanol, reaction (2). However, based on the relative rate constants of these reactions ($k_i = 2.3 \times 10^{-9}$ mol^{-1} dm^3 s^{-1} for hydroxyl radicals react with isopropanol, $k_a = 9.2 \times 10^{-6}$ mol^{-1} dm^3 s^{-1} for hydroxyl radicals react with acetic acid), this effect is expected to be quite small.[48,49] Given the magnitude of the isopropanol concentration effect, it is more likely that it can be attributed to solvent effects on the relative rates of the competing reactions. Since the isopropanol concentration effect is only observed below 1.00 M, 2.00 M of isopropanol was selected for the current study.

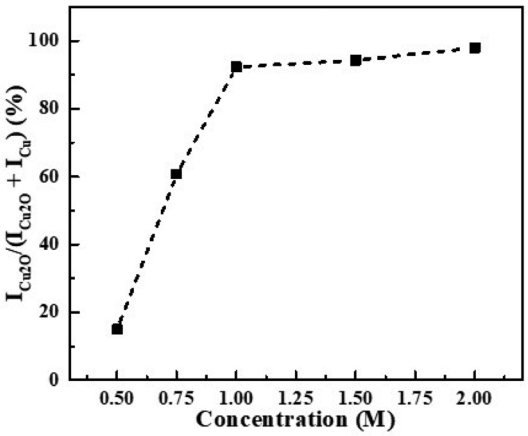

Fig. 4 The isopropanol concentration as a function of the ratios of $I_{Cu_2O}/(I_{Cu} + I_{Cu_2O})$ prepared at the solution pH 4.40. $I_{Cu_2O}/(I_{Cu} + I_{Cu_2O})$ was the ratios of integral intensities of XRD peaks, which I_{Cu_2O} and I_{Cu} represented the sum of integral intensities of peaks for Cu_2O ((110), (111), (200) and (220)) and for Cu ((111) and (200)), respectively.

It was also found that solution pH influences the morphologies of produced Cu_2O particles. SEM images of the precipitate were collected and are shown in Fig. 5(a)–(e). The Cu_2O particle size distributions obtained from the SEM images are shown in Fig. 5(f). Fig. 5(a) shows the SEM image of the metallic Cu particles obtained at pH 3.75. It was found that the Cu particles were quasi-spherical agglomerates with a 2.9 μm average size. When solution pH is increased to 3.85, two different types of particles are formed: agglomerated Cu particles and the octahedron-shaped particles which correspond to the Cu_2O phase.[7,8,14] The surfaces of the octahedrons have (111) orientation. It has been reported previously that SO_4^{2-} ions[50] and SDS[51,52] can increase the stability of {111} planes of Cu_2O which could result in the formation octahedron-shaped Cu_2O particles. As shown in Fig. 5(a)–(e), with increasing solution pH, the fraction of quasi-spherical Cu par-

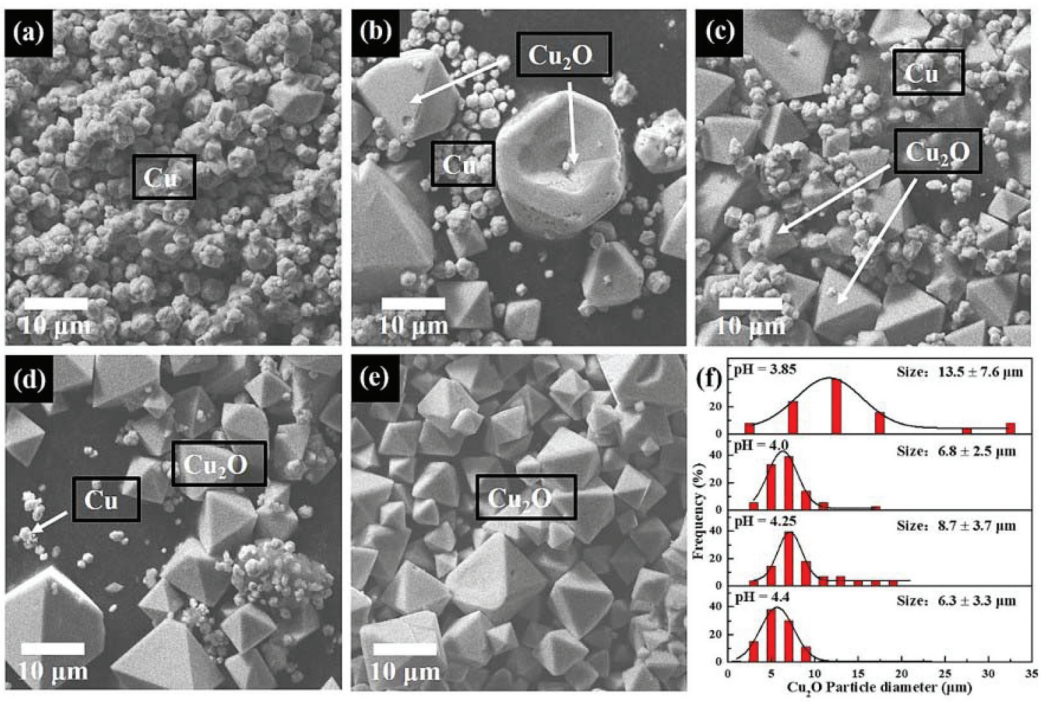

Fig. 5 SEM image of the synthesized particles by γ-radiation induced method at pH value of 3.75 (a), 3.85 (b), 4.0 (c), 4.25 (d), 4.4 (e) and the Cu_2O particles size distribution at different pH (f).

ticles is gradually decreased, whereas the Cu_2O octahedrons becomes the main phase of the produced particles. Note that the average size of the Cu_2O particles is decreased from 13.5 μm to around 7 μm (Fig. 5(f)). This could be due to the fact that at high solution pH the nucleation of Cu_2O is favorable and therefore, likely to more nucleation centers of Cu_2O are produced. This could lead to smaller particle size and likely to more narrow size distribution.[29,30,53] Solely Cu_2O particles with octahedron shape are synthesized at pH 4.40 and is shown in Fig. 5(e).

Conclusions

Cuprous oxide particles were synthesized by the reduction of dissolved Cu^{2+} ions from $CuSO_4$ aqueous solution using a γ-radiation induced synthesis route. It was found that by changing the solution pH the composition and morphology of the obtained precipitate can be tuned. Thus, at solution pH < 3.75 metallic copper quasi-spherical agglomerates are formed while at pH > 4.40 just Cu_2O octahedron-shaped particles are precipitated. In the pH range from 3.75 to 4.40, a mixture of both metallic Cu particles and Cu_2O particles are produced and the relative amount of crystalline Cu_2O in the precipitate increases with increasing pH. As a direct consequence, the overall conversion of Cu^{2+} is increased with increasing solution pH. The observed pH effect can be attributed to pH-dependent competition between the reactions yielding Cu and the reactions yielding Cu_2O. Thus, by controlling pH of the $CuSO_4$ solution during γ-radiation induced synthesis one can tune the composition and morphology of the obtained precipitate.

Conflicts of interest

There are no conflicts to declare.

Acknowledgements

The China Scholarship Council (CSC) (Grant Number: 201700260193) is gratefully acknowledged for financial support. Pavel Yushmanov is acknowledged for his help.

References

1 B. Hvolbæk, T. V. W. Janssens, B. S. Clausen, H. Falsig, C. H. Christensen and J. K. Nørskov, *Nano Today*, 2007, **2**, 14–18.
2 S. Laurent, D. Forge, M. Port, A. Roch, C. Robic, L. V. Elst and R. N. Muller, *Chem. Rev.*, 2008, **108**, 2064–2110.
3 D. A. Dinh, K. S. Hui, K. N. Hui, Y. R. Cho, W. Zhou, X. Hong and H. H. Chun, *Appl. Surf. Sci.*, 2014, **298**, 62–67.
4 S. Zinatloo-Ajabshir, M. Salavati-Niasari and M. Hamadanian, *RSC Adv.*, 2015, **5**, 33792–33800.
5 J.-Y. Ho and M. H. Huang, *J. Phys. Chem. C*, 2009, **113**, 14159–14164.
6 K. Pan, H. Ming, H. Yu, Y. Liu, Z. Kang, H. Zhang and S. T. Lee, *Cryst. Res. Technol.*, 2011, **46**, 1167–1174.
7 Y. S. Panova, A. S. Kashin, M. G. Vorobev, E. S. Degtyareva and V. P. Ananikov, *ACS Catal.*, 2016, **6**, 3637–3643.
8 X. Zhang, Y. Xie, F. Xu, X. Liu and D. Xu, *Inorg. Chem. Commun.*, 2003, **6**, 1390–1392.
9 H. B. N. Choon and Y. F. Wai, *J. Phys. Chem. B*, 2006, **110**, 20801–20807.
10 R. Wick and S. D. Tilley, *J. Phys. Chem. C*, 2015, **119**, 26243–26257.
11 Y. H. Won and L. A. Stanciu, *Sensors*, 2012, **12**, 13019–13033.
12 Y. Moglie, E. Mascaró, V. Gutierrez, F. Alonso and G. Radivoy, *J. Org. Chem.*, 2016, **81**, 1813–1818.
13 S. Kumar, C. M. A. Parlett, M. A. Isaacs, D. V. Jowett, R. E. Douthwaite, M. C. R. Cockett and A. F. Lee, *Appl. Catal., B*, 2016, **189**, 226–232.
14 H. Xu, W. Wang and W. Zhu, *J. Phys. Chem. B*, 2006, **110**, 13829–13834.
15 H. Yu, J. Yu, S. Liu and S. Mann, *Chem. Mater.*, 2007, **19**, 4327–4334.
16 M. Wang, L. Xu, M. Zhai, J. Peng, J. Li and G. Wei, *Carbohydr. Polym.*, 2008, **74**, 498–503.
17 D. Wu, X. Ge, Y. Huang, Z. Zhang and Q. Ye, *Mater. Lett.*, 2003, **57**, 3549–3553.
18 P. A. Yakabuskie, J. M. Joseph, P. Keech, G. A. Botton, D. Guzonas and J. C. Wren, *Phys. Chem. Chem. Phys.*, 2011, **13**, 7198.
19 D. C. Clifford, C. E. Castano and J. V. Rojas, *Radiat. Phys. Chem.*, 2017, **132**, 52–64.
20 I. L. Soroka, N. V. Tarakina, A. Hermansson, L. Bigum, R. Widerberg, M. S. Andersson, R. Mathieu, A. R. Paulraj and Y. Kiros, *Dalton Trans.*, 2017, **46**, 9995–10002.
21 M. E. Meyre, M. Tréguer-Delapierre and C. Faure, *Langmuir*, 2008, **24**, 4421–4425.
22 J. Vinod Kumar, N. Lingaiah, K. S. Rama Rao, S. P. Ramnani, S. Sabharwal and P. S. Sai Prasad, *Catal. Commun.*, 2009, **10**, 1149–1152.
23 H. Wang, X. Sun, Y. Ye and S. Qiu, *J. Power Sources*, 2006, **161**, 839–842.
24 J. W. T. Spinks and R. J. Woods, *An introduction to Radiation Chemistry*, Wiley, New York-London-Sydney, 1990.
25 S. Bzdon, J. Góralski, W. Maniukiewicz, J. Perkowski, J. Rogowski and M. Szadkowska-Nicze, *Radiat. Phys. Chem.*, 2012, **81**, 322–330.
26 O. Roth, H. Hasselberg and M. Jonsson, *J. Nucl. Mater.*, 2009, **383**, 231–236.
27 L. M. Alrehaily, J. M. Joseph, A. Y. Musa, D. A. Guzonas and J. C. Wren, *Phys. Chem. Chem. Phys.*, 2013, **15**, 98–107.
28 L. M. Alrehaily, J. M. Joseph and J. C. Wren, *J. Phys. Chem. C*, 2015, **119**, 16321–16330.
29 P. He, X. Shen and H. Gao, *J. Colloid Interface Sci.*, 2005, **284**, 510–515.
30 H. Liu, W. Miao, S. Yang, Z. Zhang and J. Chen, *Cryst. Growth Des.*, 2009, **9**, 1733–1740.

31 S. Das and V. C. Srivastava, *Mater. Lett.*, 2015, **150**, 130–134.
32 K. Okitsu, K. Sharyo and R. Nishimura, *Langmuir*, 2009, **25**, 7786–7790.
33 A. P. A. Faiyas, E. M. Vinod, J. Joseph, R. Ganesan and R. K. Pandey, *J. Magn. Magn. Mater.*, 2010, **322**, 400–404.
34 X. Li, W. X. Chen, J. Zhao, W. Xing and Z. De Xu, *Carbon*, 2005, **43**, 2168–2174.
35 A. V. Nikam, A. Arulkashmir, K. Krishnamoorthy, A. A. Kulkarni and B. L. V. Prasad, *Cryst. Growth Des.*, 2014, **14**, 4329–4334.
36 T. M. D. Dang, T. T. T. Le, E. Fribourg-Blanc and M. C. Dang, *Adv. Nat. Sci.: Nanosci. Nanotechnol.*, 2011, **2**, 015009.
37 F. S. Ohuchi, T. J. Lin, J. A. Antonelli and D. J. Yang, *Mater. Res. Bull.*, 1994, **6090**, 10–16.
38 A. Mozumder, *Fundamentals of Radiation Chemistry*, Academic Press, USA, 1999.
39 H. A. Schwarz, *J. Chem. Educ.*, 1981, **58**, 101.
40 G. R. Dey, *Radiat. Phys. Chem.*, 2005, **74**, 172–184.
41 R. E. Huie, C. L. Clifton and P. Neta, *Int. J. Radiat. Appl. Instrum. Part*, 1991, **38**, 477–481.
42 I. L. Soroka, A. Shchukarev, M. Jonsson, N. V. Tarakina and P. A. Korzhavyi, *Dalton Trans.*, 2013, **42**, 9585.
43 A. Karelovic and P. Ruiz, *Catal. Sci. Technol.*, 2015, **5**, 869–881.
44 D. Vargas-Hernández, J. M. Rubio-Caballero, J. Santamaría-González, R. Moreno-Tost, J. M. Mérida-Robles, M. A. Pérez-Cruz, A. Jiménez-López, R. Hernández-Huesca and P. Maireles-Torres, *J. Mol. Catal. A: Chem.*, 2014, **383–384**, 106–113.
45 I. V. Korolkov, O. Güven, A. A. Mashentseva, A. B. Atıcı, Y. G. Gorin, M. V. Zdorovets and A. A. Taltenov, *Radiat. Phys. Chem.*, 2017, **130**, 480–487.
46 J. M. Steigerwald, S. P. Murarka, R. J. Gutmann and D. J. Duquette, *Mater. Chem. Phys.*, 1995, **41**, 217–228.
47 Q. Chen, X. Shen and H. Gao, *J. Colloid Interface Sci.*, 2007, **312**, 272–278.
48 A. J. Elliot and A. S. Simsons, *Radiat. Phys. Chem.*, 1984, **24**, 229–231.
49 J. K. Thomas, *Trans. Faraday Soc.*, 1965, **61**, 702–707.
50 M. J. Siegfried and K. S. Choi, *J. Am. Chem. Soc.*, 2006, **128**, 10356–10357.
51 M. J. Siegfried and K. S. Choi, *Angew. Chem.,Int. Ed.*, 2005, **44**, 3218–3223.
52 M. J. Siegfried and K. S. Choi, *Adv. Mater.*, 2004, **16**, 1743–1746.
53 J. Belloni, *Catal. Today*, 2006, **113**, 141–156.